Delft University of Technology

Microstructure and hardness of SAC305-xNi solder on Cu and graphene-coated Cu substrates

Liu, Yang; Li, Shengli; Zhang, Hao; Cai, Hongming; Sun, Fenglian; Zhang, Guoqi

DOI
10.1007/s10854-018-9440-2

Publication date
2018

Document Version
Final published version

Published in
Journal of Materials Science: Materials in Electronics

Citation (APA)
Liu, Y., Li, S., Zhang, H., Cai, H., Sun, F., & Zhang, G. (2018). Microstructure and hardness of SAC305-xNi solder on Cu and graphene-coated Cu substrates. *Journal of Materials Science: Materials in Electronics*, *29*(15), 13167-13175. https://doi.org/10.1007/s10854-018-9440-2

Important note
To cite this publication, please use the final published version (if applicable).
Please check the document version above.

Copyright
Other than for strictly personal use, it is not permitted to download, forward or distribute the text or part of it, without the consent of the author(s) and/or copyright holder(s), unless the work is under an open content license such as Creative Commons.

Takedown policy
Please contact us and provide details if you believe this document breaches copyrights.
We will remove access to the work immediately and investigate your claim.

This work is downloaded from Delft University of Technology.
For technical reasons the number of authors shown on this cover page is limited to a maximum of 10.

Journal of Materials Science: Materials in Electronics (2018) 29:13167–13175
https://doi.org/10.1007/s10854-018-9440-2

Microstructure and hardness of SAC305-xNi solder on Cu and graphene-coated Cu substrates

Yang Liu[1,2] · Shengli Li[1] · Hao Zhang[1,2] · Hongming Cai[1] · Fenglian Sun[1] · Guoqi Zhang[2]

Received: 28 March 2018 / Accepted: 8 June 2018 / Published online: 9 June 2018
© Springer Science+Business Media, LLC, part of Springer Nature 2018

Abstract

This study investigated the interfacial reaction, the microstructure, and the hardness of the SAC305-xNi solder on both Cu and graphene-coated Cu (G–Cu) substrates. The experimental results indicate that the increase of Ni content in the solder leads to the roughness of the $(Cu, Ni)_6Sn_5$ IMC layer on Cu. In contrast, the growth of the $(Cu, Ni)_6Sn_5$ interfacial IMC, which results from increasing Ni addition, is significantly suppressed on G–Cu substrates. As the concentration of Ni ranges from 0 to 0.2 wt%, the microstructure of the solder bulks on Cu substrates shows slight changes. The hardness of the solder bulks in SAC305-Ni/Cu is similar to that in the SAC305/Cu solder joint. The amount of β-Sn rises and the eutectic area shrinks due to increasing Ni addition in the solder bulks on G–Cu substrates. Therefore, the solder bulks in the SAC305-Ni/G–Cu show lower hardness than that in the SAC305/G–Cu solder joint.

1 Introduction

As the development of electronics technology, high integration, high performance, and miniaturization are dominated trends for electrical products [1–3]. The miniaturization of solder joints has brought a series of reliability issues which affect the life time of products. The roughness of interfacial intermetallic compounds (IMC) is considered as one of the key factors that lead to the deterioration of the reliability of solder joints [4–6].

Cu is the most common pad material on substrates. Deng et al. [7] studied the shear strength and the fracture behavior of Sn3.5Ag/Cu solder joints during reflow and thermal aging. It is suggested that the growth of interfacial IMC layers, such as Cu_6Sn_5 and Cu_3Sn in the solder joints on Cu, leads to the interfacial brittleness. Besides, Zeng et al. [8] observed a large number of Kirkendall voids at the interface between Cu_3Sn and Cu in their research. The formation of Kirkendall voids are also considered as the reason for the reliability degradation of solder joints. One of the ways to suppress IMC roughness is to conduct surface treatment on Cu. Pan and Hsieh [9] used Co (W, P) as the diffusion barrier for SnAgCu (SAC) solder joints. It was found that the concentrations of W and P have significant effects on the IMC growth and the bonding strength. Zou et al. [10] found that the Cu_6Sn_5 IMC showed different morphologies and growth rates on the (0 0 1), (0 1 1), (1 1 1) and (1 2 3) Cu single crystals. Adawiyah and Azlina [11] developed a new electroless nickel/immersion silver (ENImAg) surface finish. The ENImAg surface finish reduces the growth rate and the grain size of interfacial IMCs on Cu substrate. Ko et al. [12] prepared graphene-coated Cu substrate by a layer-by-layer transfer process. According to their study, graphene layer has positive effects on suppressing the coarsening of interfacial IMC layers in solder joints. Therefore, it is possible to optimize the microstructure and the mechanical properties of solder joints by surface treatment of Cu substrates.

Another common method to decrease the growth rate of IMC is to add minor elements into solder materials [13–16]. Wang et al. [17] indicated that the grain size of β-Sn decreased when 0.2 wt% Zn was added into the Sn0.7Cu solder. Meanwhile, the growth of Cu_6Sn_5 and Cu_3Sn layers were suppressed. As Zn content reached 1 wt% in the solder alloy, the interfacial IMC transformed from Cu_6Sn_5 to CuZn and thus decreased the growth rate of IMC during the high temperature aging test. Wang et al. [18] used Co and Ni as the adding elements into the Sn-based solder alloys. Because Co and Ni have similar atom size with Cu, Cu atoms in the

✉ Yang Liu
lyang805@163.com

[1] School of Materials Science and Engineering, Harbin University of Science and Technology, Harbin 150040, People's Republic of China

[2] EEMCS Faculty, Delft University of Technology, Delft, The Netherlands

IMC of Cu_6Sn_5 will be replaced and thus form the IMC of $(Cu, Ni)_6Sn_5$ or $(Cu, Co)_6Sn_5$. Liu et al. [19] compared the growth behavior of IMCs between SAC305 and SAC0705-BiNi solder joints. The results revealed that the addition of Ni significantly suppressed the growth of Cu_3Sn layer and the formation of Kirkendall voids. The outstanding performances of graphene promote the application of this material in various fields including soldering. Hu et al. [20] added 0.1 wt% graphene into Sn8Zn3Bi solder alloy. Graphene is located at the interface of solder joint and suppresses the interfacial diffusion under thermal and electrical fields. The growth rate of Cu_5Zn_8 interfacial IMC decreases from 30.9×10^{14} to 24.9×10^{14} cm^2/s. Meanwhile, Xu et al. [21] demonstrated that the addition of graphene in SAC305 solder showed positive effects on suppressing the roughness of Cu_6Sn_5 interfacial IMC.

In this study, graphene was coated onto the surface of Cu substrates by chemical vapor deposition (CVD) method. SAC305-xNi solder alloys were soldered onto graphene-coated Cu (G–Cu) substrates and normal Cu substrates. The interfacial IMC, the microstructure of the solder bulk, and the hardness of the solder joints were investigated.

2 Experimental procedure

SAC305-xNi solder alloys were obtained by a melting process with the protective air of N_2. Here the concentration of Ni was 0, 0.05, 0.1, and 0.2 wt%, respectively. Then the solder bulks were made into solder balls with the diameter of 1.6 mm. The substrates used in this study included common Cu substrates and G–Cu substrates. The preparation process of G–Cu substrates was as follow: firstly, the Cu substrate was heated up to 1000 °C in an oven with the gases of Ar (300 sccm) and H_2 (50 sccm) for 30 min. Secondly, CH_4 (5 sccm), Ar (500 sccm), and H_2 (50 sccm) were released into the oven for 8 min. At last, the substrate was cooled in the oven with the protection of Ar (300 sccm) and H_2 (50 sccm) gases. In order to characterize the two types of substrates, Raman spectroscopy and XRD tests were conducted. The Raman patterns shown in Fig. 1 reveal that graphene layer is successfully coated on G–Cu substrates.

The SAC305-xNi solder balls were soldered onto Cu and G–Cu substrates with the peak temperature of 260 °C for 60 s using a commercial AMTECH flux. The wetting area of each solder joint was measured to evaluate its solderability. Cross-sectional specimens of these solder joints were obtained after embedding and mechanical polishing steps. The microstructure of the solder bulks were observed by metallographic optical microscope and SEM. Meanwhile, the morphology of the interfacial IMC layers of these solder joints were obtained. The composition of the solder bulks and IMC layers were characterized by EDS. DUH-211S indentation equipment was employed to evaluate the hardness of the solder bulks on both Cu and G–Cu substrates. The max load used in the indentation test was 20 mN.

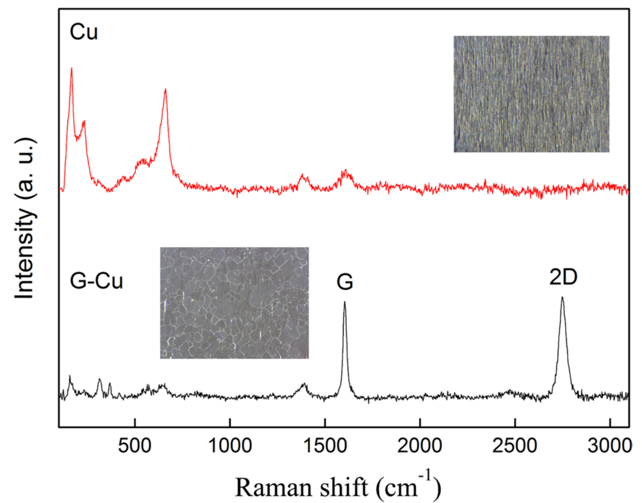

Fig. 1 Raman analysis of Cu and G–Cu substrates

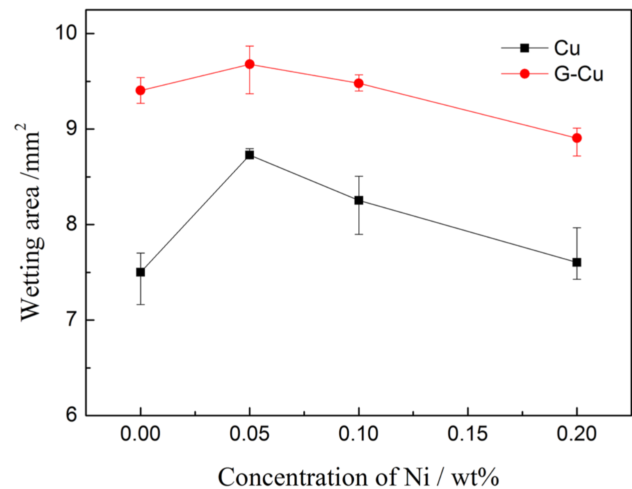

Fig. 2 Wetting area of the SAC305-xNi solders on the two substrates

3 Results and discussion

3.1 Solderability of the solder alloys

Figure 2 displays the wetting area of SAC305-xNi solder spheres on Cu and G–Cu substrates. The wetting areas on the two substrates show similar trends due to the increasing Ni content in the solder alloys. When the concentration of Ni is 0.05 wt%, the wetting areas are improved on both Cu and G–Cu substrates. Further Ni addition leads to the degradation of the solderability of the solder alloys. According to

our previous findings, the interfacial IMC transforms from Cu_6Sn_5 into $(Cu, Ni)_6Sn_5$ with 0.05 wt% Ni addition in the solder [22]. Such transformation is considered as the reason for the improvement of solderability. However, Cheng et al. [23] indicated that the increasing concentration of elements like Co and Ni in the solder alloys causes the solid IMCs formation in the molten solders during reflow. Thus the fluidity and solderability of the solder alloys decreases. By comparing the wetting areas of the SAC305-xNi solder alloys on the two substrates, it is obvious that the solderability of the solder on G–Cu substrate is much higher than that on Cu substrate. As indicated in Fig. 1, the surface morphology and the structure of the Cu substrate change during the graphene-coating process. This may be a possible reason for the enhancement of solderability. More importantly, Chen et al. [24] revealed that the oxidation of Cu can be significantly suppressed by the graphene-coated layer. This is suggested to be the governing mechanism for the solderability improvement. Additionally, Huang et al. [25] indicated that trace amount addition of graphene improved the solderability of SAC solder. In this study, there is a possibility that some of the graphene dissolved into the molten solder during soldering process and thus affected the solderability.

3.2 Interfacial IMC layers in the solder joints

Figure 3 shows the SEM morphology of the interfacial IMCs in the SAC305-xNi/Cu interfaces. As shown in Fig. 3a, the interfacial IMC between SAC305 and Cu is typical scallop-like Cu_6Sn_5. Figure 3b–d show the morphology of IMCs in the solder joints of SAC305-xNi/Cu with Ni content of 0.05, 0.1, and 0.2 wt%, respectively. With the addition of Ni element in the SAC305 solder, it is clear that the composition of the interfacial IMC transforms from Cu_6Sn_5 into $(Cu, Ni)_6Sn_5$. The grain size of the $(Cu, Ni)_6Sn_5$ phase is significantly smaller than that of the Cu_6Sn_5 IMC. As explained in the publication [26], Ni atoms in the solder alloys replaces some of the Cu atoms in Cu_6Sn_5 and thus forms $(Cu, Ni)_6Sn_5$. Compared with Cu_6Sn_5, $(Cu, Ni)_6Sn_5$ has more nucleation sites. Consequently, the $(Cu, Ni)_6Sn_5$ IMC layer has smaller grain size than the Cu_6Sn_5 interfacial layer does. However, the increasing amount of nucleation sites in $(Cu, Ni)_6Sn_5$ promotes the formation of $(Cu, Ni)_6Sn_5$ grains. Therefore, the thickness of the $(Cu, Ni)_6Sn_5$ layers increases because of the ascending amount of the $(Cu, Ni)_6Sn_5$ grains. As shown in Fig. 3b–d, the thickness of the $(Cu, Ni)_6Sn_5$ IMC layer increases obviously when

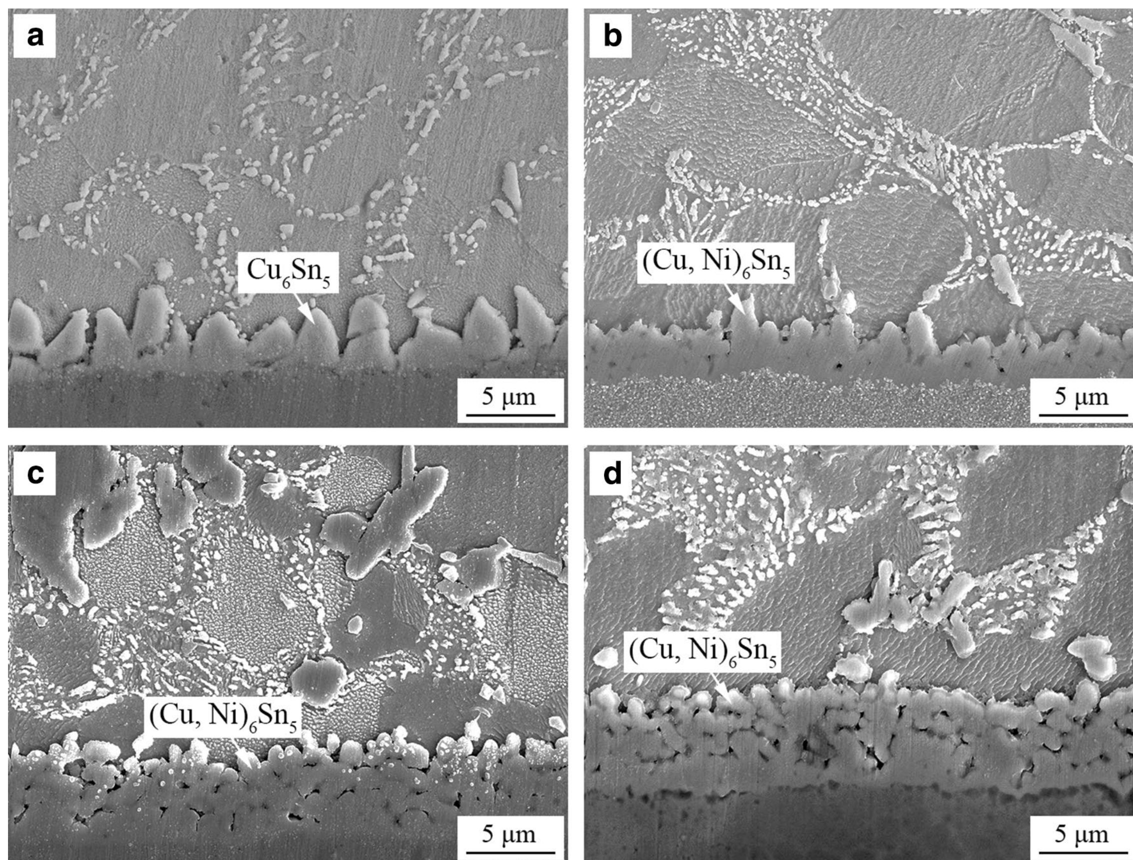

Fig. 3 SEM morphology of the interfacial IMCs on Cu substrate: **a** SAC305, **b** SAC305-0.05Ni, **c** SAC305-0.1Ni, **d** SAC305-0.2Ni

the concentration of Ni rises from 0.05 to 0.1 wt% in the SAC305-xNi solders.

The SEM morphology of the interfacial IMCs in SAC305-xNi/G-Cu solder joints is as shown in Fig. 4. As presented in Fig. 3a, the interfacial IMC in SAC305/G–Cu is scallop Cu_6Sn_5. The morphology of this IMC layer is similar to the Cu_6Sn_5 IMC in the SAC305/Cu solder joints in Fig. 3a. As shown in Fig. 4b–d, the IMC layers show a smooth interface between the IMC layers and the solder bulks in the SAC305-xNi/G–Cu solder joints when Ni content ranges from 0.05 to 0.2 wt%. The EDS results presented in Fig. 5 demonstrate that the composition of the IMC layers are $(Cu, Ni)_6Sn_5$. Compared with the $(Cu, Ni)_6Sn_5$ IMC layers on Cu substrates in Fig. 3b–d, the $(Cu, Ni)_6Sn_5$ on G–Cu substrate has thinner thickness and smoother morphology.

Figure 6 shows the thickness of each IMC layer of SAC305-xNi solder on Cu and G–Cu substrates. As shown in the figure, the thickness of Cu_6Sn_5 on the Cu substrate is about 3.2 µm when the concentration of Ni is 0 in the solder. With the addition of Ni by 0.05 wt% in the solder, the IMC layer transforms to $(Cu, Ni)_6Sn_5$, and the thickness of the IMC layer decreases to 2.9 µm. As the concentration of Ni reaches 0.1 and 0.2 wt% in the solder alloys, the thickness of the IMC $(Cu, Ni)_6Sn_5$ layers increases obviously and reaches 4.9 and 5.2 µm respectively. According to the thickness showed in the figure, it is evident that the IMC layers on the G–Cu have thinner thickness than that on the Cu substrate when the x varies from 0 to 0.2 in the SAC305-xNi solder. Here the thickness of the IMC layers on the G–Cu substrate shows a slow ascending trend and mainly ranges from 1.7 to 2.4 µm due to the increase of Ni content. There are two possible reasons to explain this phenomenon that the IMC layer is thinner on the G–Cu substrate than that on the Cu substrate. Firstly, the XRD patterns in Fig. 7 illustrates that the crystal structure of Cu transforms from polycrystalline into (200) single crystal structure after the graphene-coating process. The growth of the IMC layers during the soldering process is suppressed. Secondly, as reported by Hu et al. [20] and Xu et al. [21], graphene also plays a role in suppressing the growth and the roughness of interfacial IMC layers.

3.3 Microstructure and hardness of the solder bulks in the solder joints

Figure 8 presents the microstructure of the solder bulks on Cu substrates by optical microscope. As shown in Fig. 8a,

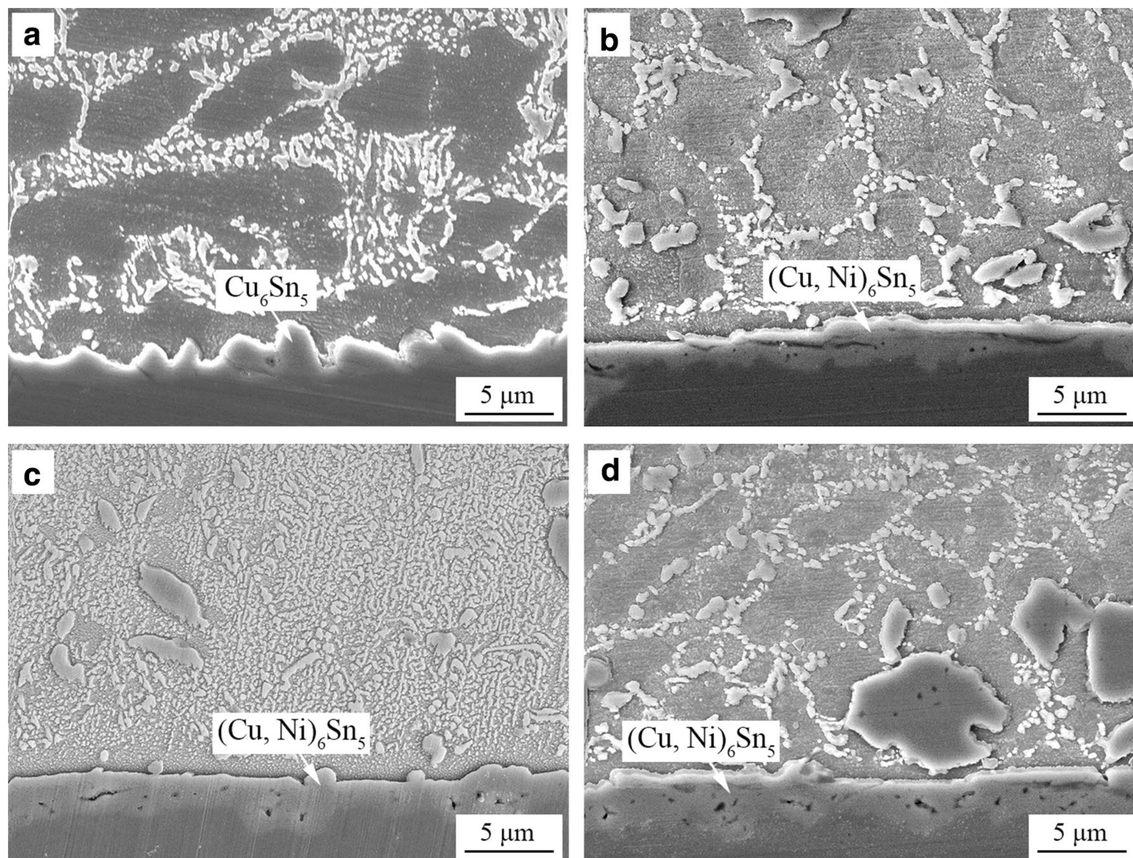

Fig. 4 SEM morphology of the interfacial IMCs on G–Cu substrate: **a** SAC305, **b** SAC305-0.05Ni, **c** SAC305-0.1Ni, **d** SAC305-0.2Ni

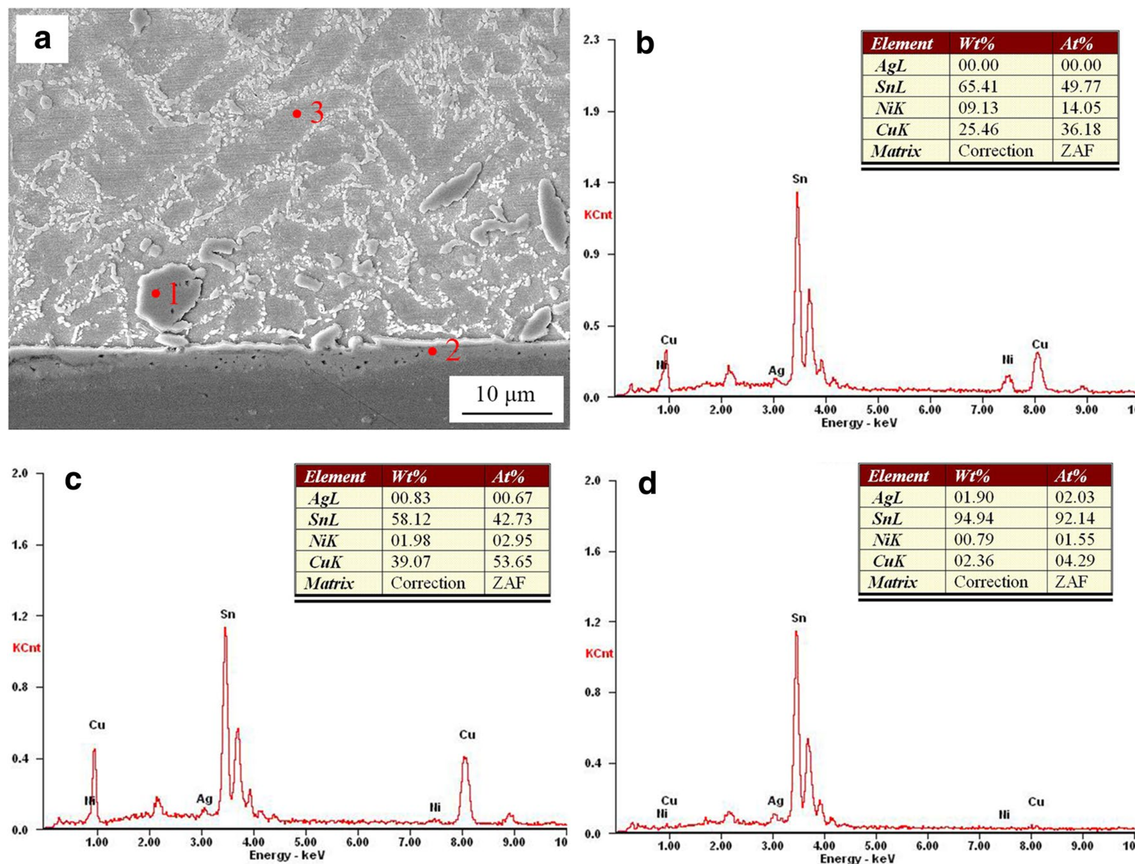

Fig. 5 SEM and EDS of SAC305-0.2Ni/G-Cu solder joint: **a** SEM morphology, **b** EDS of point 1, **c** EDS of point 2, **d** EDS of point 3

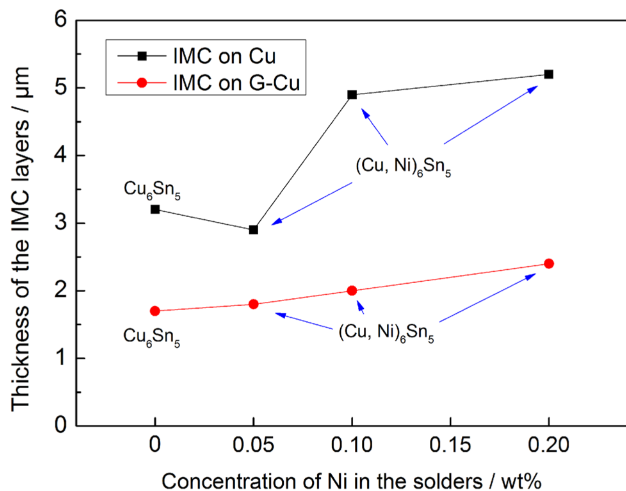

Fig. 6 Thickness of the IMC layers in the solder joints

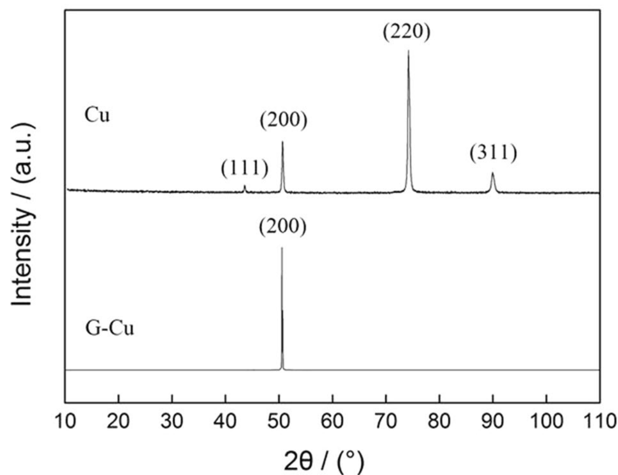

Fig. 7 XRD patterns of Cu and G–Cu substrates

the solder bulk in the SAC305/Cu solder joint includes two parts, the β-Sn and the eutectic area. As the addition of Ni content in the solder alloys, $(Cu, Ni)_6Sn_5$ IMC phase appears in the solder bulks as shown in Fig. 8b–d. In contrast, the increasing concentration of Ni shows limited effects on the morphology of β-Sn and the eutectic area in the solder bulks.

As shown in Fig. 9, the solder bulks on G–Cu substrates display quite different microstructure from the solder bulks on the Cu substrate. For the SAC305/G–Cu solder joint, the

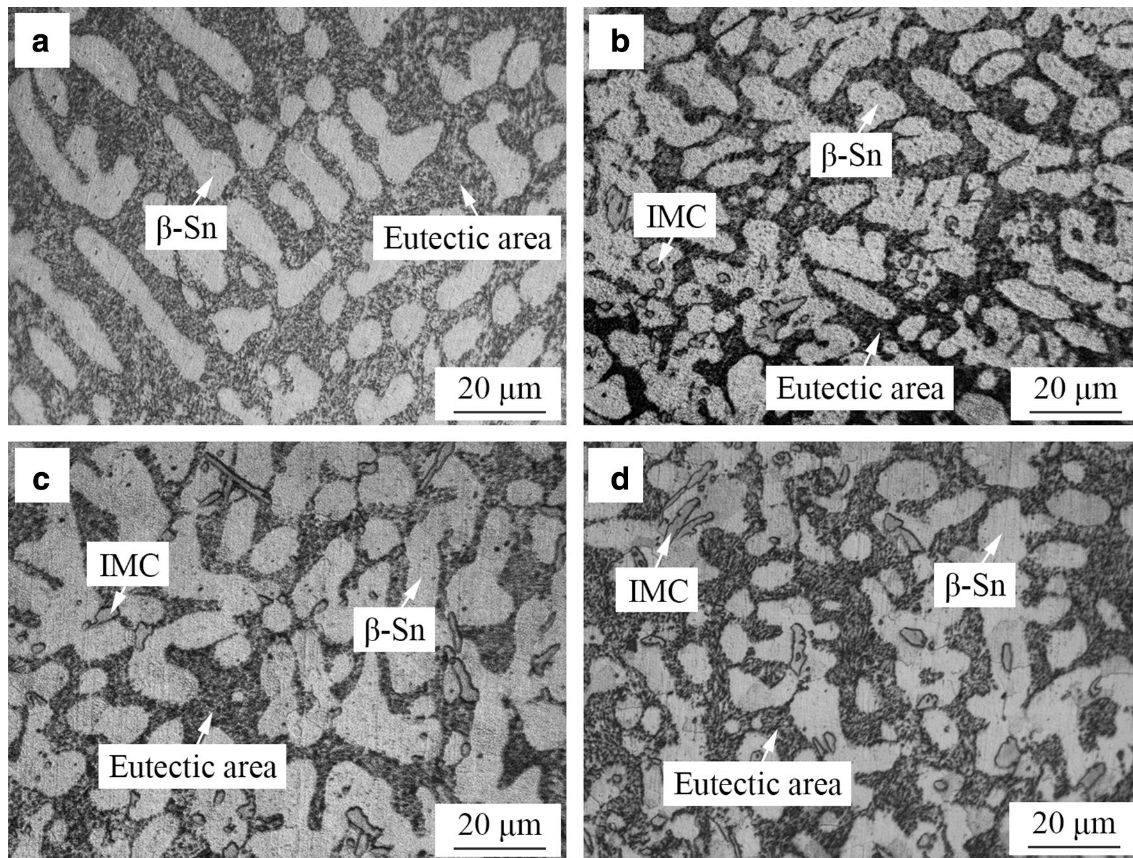

Fig. 8 Microstructure of the solder bulks on Cu substrate: **a** SAC305, **b** SAC305-0.05Ni, **c** SAC305-0.1Ni, **d** SAC305-0.2Ni

β-Sn and the eutectic area are the main parts which form the solder bulk. Compared with the microstructure of SAC305 on the Cu substrate as shown in Fig. 8a, the morphology of the β-Sn grains on the G–Cu substrate is smaller. This phenomenon demonstrates that the graphene-coating treatment on Cu substrates does not only affect the morphology of the interfacial IMC layer, but also has some influences on the microstructure of the solder bulk. Such effect on the solder bulks is even significant when Ni is doped into the solder alloy. As shown in Fig. 9b–d, it is obvious that the microstructure of the solder bulks transforms due to the addition of Ni. As Ni content rises from 0.05 to 0.2 wt% in the solder alloys, the amount of β-Sn grains increases but the area of the eutectic phase decreases.

In order to discuss the effect of the substrates on the solder bulks, magnified SEM micrographs are shown in Fig. 10. As illustrated in Fig. 10a, b, the area of the eutectic phase is similar in the microstructure of SAC305 and SAC305-0.2Ni on Cu substrates. According to the study of the interfacial IMC layers as shown in Fig. 2, the increase of Ni content mainly takes part in the interfacial reaction of the formation and the growth of the $(Cu, Ni)_6Sn_5$ interfacial layers. In contrast, the effect of Ni on the microstructure of the solder bulks is limited. For the solders on the G–Cu substrate, however, the situation is different. As presented in Fig. 4b–d, the increase of the concentration of Ni has a limited influence on the morphology of the $(Cu, Ni)_6Sn_5$ interfacial layers. This means that more Ni atoms take part in the formation of the microstructure of the solder bulks on the G–Cu substrate with increasing Ni concentration in the solder alloys. Consequently, the formation of the eutectic phase is suppressed and the eutectic area shrinks as shown in Fig. 10c, d.

The hardness of the solder bulks of SAC305-xNi on Cu and G–Cu substrates are as shown in Figs. 11 and 12, respectively. In order to have an overall evaluation of the solder bulks, the indentation tests were conducted at various positions including the top, the middle, and the bottom areas on each solder bulk. As presented in Fig. 11, the increase of Ni concentration in the solder alloys has limited effects on the hardness of the SAC305-xNi solder bulks on Cu substrates. The hardness of the solder bulks are about 200 to 240 MPa when the concentration of Ni ranges from 0 to 0.2 wt% in the solders. Figure 12 demonstrates the hardness variation due to the increase of Ni concentration in the solders on the G–Cu substrate. As shown in the figure, the addition of Ni in the solder alloys leads to a decrease trend of the hardness

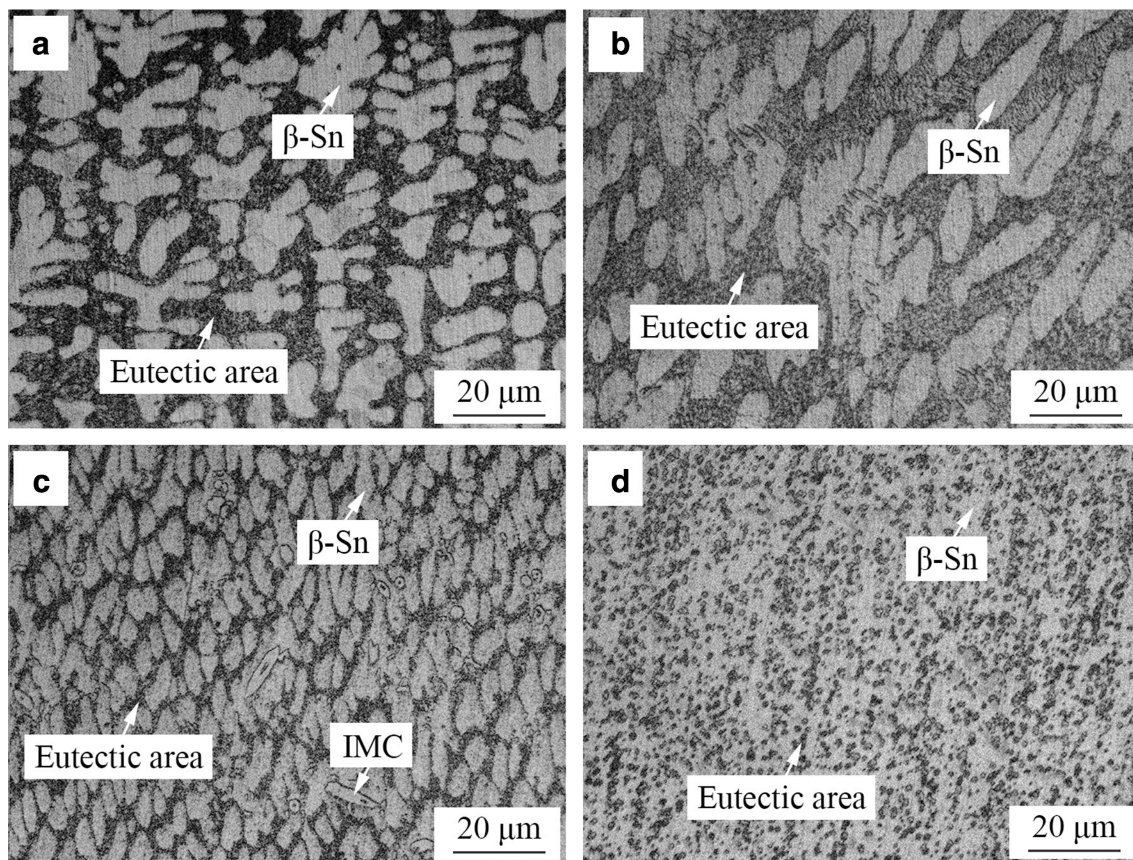

Fig. 9 Microstructure of the solder bulks on G–Cu substrate: **a** SAC305, **b** SAC305-0.05Ni, **c** SAC305-0.1Ni, **d** SAC305-0.2Ni

of the solder bulks. Here the hardness of SAC305 is about 200 to 250 MPa on the G–Cu substrate. Due to the addition of Ni, the hardness of SAC305-0.2Ni solder bulk drops to about 150 MPa. As presented in Figs. 8, 10a, b, the Ni-doped solders and SAC305 have similar areas of the eutectic phase on Cu substrates. Therefore, Ni addition has limited effects on the hardness of the solder bulks on Cu substrates. However, as shown in Figs. 9, 10c, d, the amount of β-Sn increases but the eutectic area decreases in the solder bulks due to Ni addition in the solders on G–Cu substrates. Since β-Sn is approved to be a soft phase, the increasing amount of β-Sn is suggested as the dominating factor for the decline of the hardness. Another phenomenon is that the hardness of SAC305-xNi solder bulks on G–Cu is lower than that on Cu. As shown in Figs. 8, 9, and 10, the β-Sn phase in the solder bulks on G–Cu show smaller grain size and larger amount than that on Cu. As discussed above, there is a possibility that some of the graphene dissolved into the molten solder during soldering process. According to the research by Huang et al. [25], the minor addition of graphene leads to the refinement of the microstructure of solder bulk. Therefore, the solder bulks of SAC305-xNi on G–Cu show lower hardness than that on Cu substrate.

4 Conclusions

1. The interfacial IMC is scallop-like Cu_6Sn_5 in both SAC305/Cu and SAC305/G–Cu solder joints. The addition of Ni element leads to a transformation from Cu_6Sn_5 to $(Cu, Ni)_6Sn_5$ on both Cu and G–Cu substrates.
2. As the concentration of Ni increases from 0.05 to 0.2 wt% in the solder alloys, the $(Cu, Ni)_6Sn_5$ IMC on Cu substrates appears obvious roughness. In contrast, the increasing amount of Ni has limited effects on the growth of the $(Cu, Ni)_6Sn_5$ interfacial IMC layer on G–Cu substrates.
3. The microstructure of the solder bulks is similar in the SAC305/Cu and the SAC-Ni/Cu solder joints. Consequently, the effect of Ni addition in the SAC305 solder exerts slight influences on the hardness of solder bulks.
4. As the increase of Ni addition, the amount of β-Sn rises but the eutectic area declines in the solder bulks on G–Cu substrates. As a result, the hardness of the solder bulks on G–Cu substrates drops due to the addition of Ni in solder alloys.

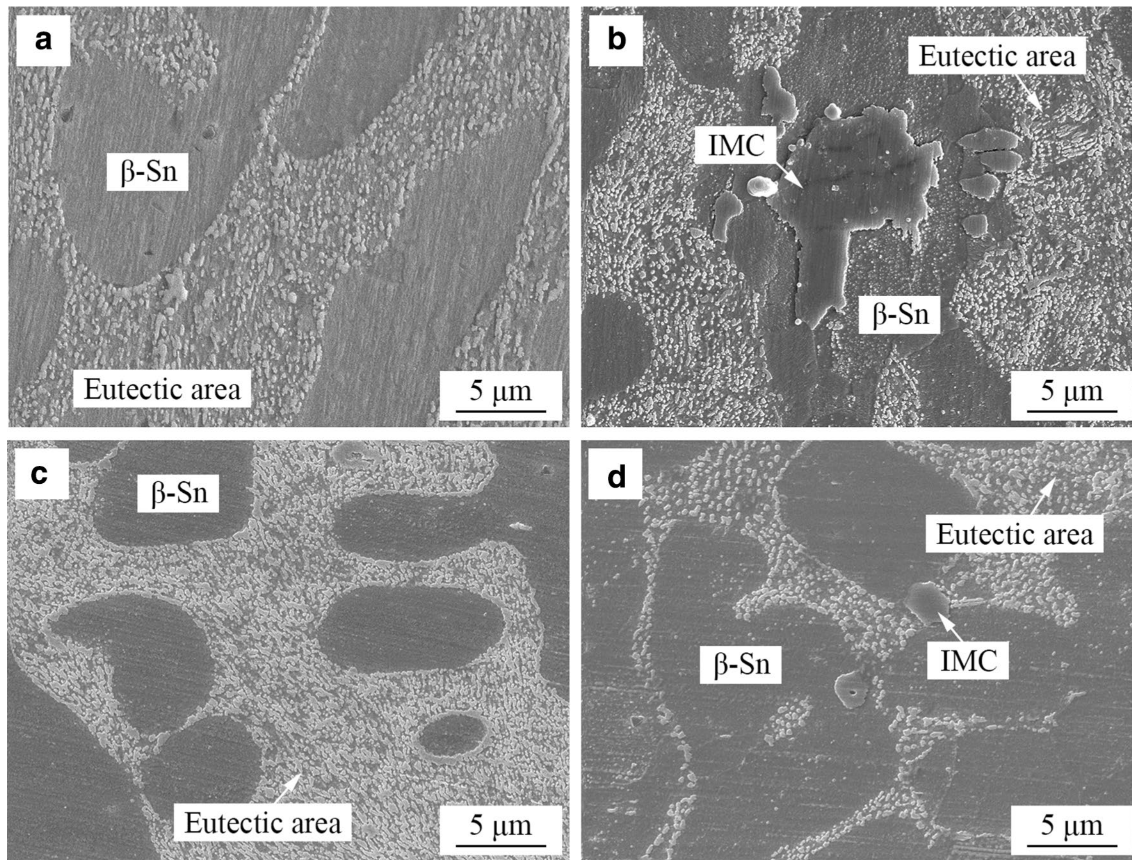

Fig. 10 Magnified microstructure of the solder bulks by SEM: **a** SAC305 on Cu, **b** SAC305-0.2Ni on Cu, **c** SAC305 on G–Cu, **d** SAC305-0.2Ni on G–Cu

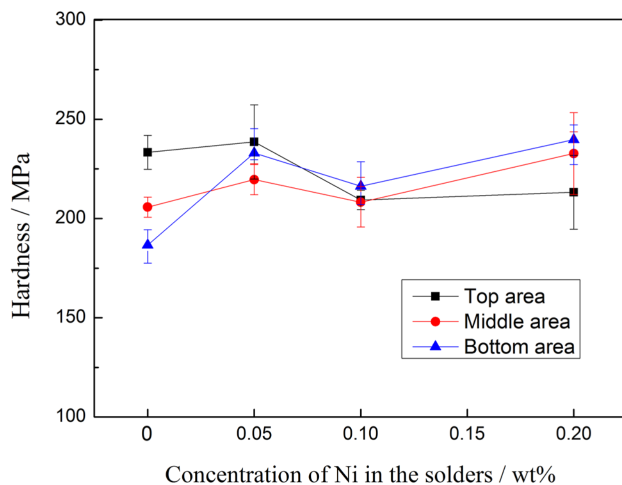

Fig. 11 Hardness of the solder bulks of SAC305-xNi/Cu

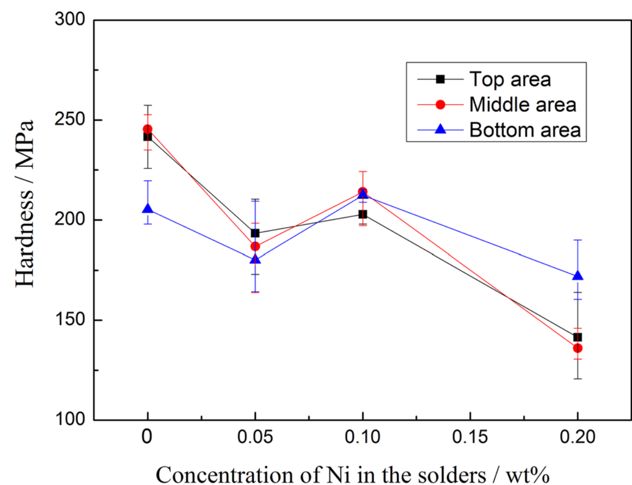

Fig. 12 Hardness of the solder bulks of SAC305-xNi/G–Cu

Acknowledgements This work is supported by National Natural Science Foundation of China (No. 51604090), Natural Science Foundation of Heilongjiang Province (No. E2017050), and University Nursing Program for Young Scholars with Creative Talents in Heilongjiang Province (UNPYSCT-2015042).

References

1. J. Kim, A. Banks, Z. Xie, S.Y. Heo, P. Gutruf, J.W. Lee, S. Xu, K.I. Jang, F. Liu, G. Brown, Miniaturized flexible electronic

systems with wireless power and near-field communication capabilities. Adv. Funct. Mater. **25**, 4761–4767 (2015)

2. N.A. Kyeremateng, T. Brousse, D. Pech, Microsupercapacitors as miniaturized energy-storage components for on-chip electronics. Nat. Nanotechnol. **12**, 7 (2017)
3. M. Shtein, R. Nadiv, M. Buzaglo, O. Regev, Graphene-based hybrid composites for efficient thermal management of electronic devices. ACS Appl. Mater. Int. **7**, 23725–23730 (2015)
4. Y. Liu, F. Sun, L. Luo, C.A. Yuan, G. Zhang, Microstructure evolution and shear behavior of the solder joints for flip-chip LED on ENIG substrate. J. Electron. Mater. **44**, 2450–2457 (2015)
5. X. Ma, Y. Qian, F. Yoshida, Effect of La on the Cu–Sn intermetallic compound (IMC) growth and solder joint reliability. J. Alloys Compd. **334**, 224–227 (2002)
6. J.H. Pang, T. Low, B. Xiong, X. Luhua, C. Neo, Thermal cycling aging effects on Sn–Ag–Cu solder joint microstructure, IMC and strength. Thin Solid Films **462**, 370–375 (2004)
7. X. Deng, R. Sidhu, P. Johnson, N. Chawla, Influence of reflow and thermal aging on the shear strength and fracture behavior of Sn-3.5Ag solder/Cu joints. Metall. Mater. Trans. A **36**, 55–64 (2005)
8. K. Zeng, R. Stierman, T.C. Chiu, D. Edwards, K. Ano, K. Tu, Kirkendall void formation in eutectic SnPb solder joints on bare Cu and its effect on joint reliability. J. Appl. Phys. **97**, 024508 (2005)
9. H.C. Pan, T.E. Hsieh, Diffusion barrier characteristics of electroless Co (W, P) thin films to lead-free SnAgCu solder. J. Electrochem. Soc. **158**, P123–P129 (2011)
10. H. Zou, Q. Zhu, Z. Zhang, Growth kinetics of intermetallic compounds and tensile properties of Sn–Ag–Cu/Ag single crystal joint. J. Alloys Compd. **461**, 410–417 (2008)
11. M.R. Adawiyah, O.S. Azlina, Comparative study on the isothermal aging of bare Cu and ENImAg surface finish for Sn-Ag-Cu solder joints. J. Alloys Compd. **740**, 958–966 (2018)
12. Y.H. Ko, J.D. Lee, T. Yoon, C.W. Lee, T.S. Kim, Controlling interfacial reactions and intermetallic compound growth at the interface of a lead-free solder joint with layer-by-layer transferred graphene. ACS Appl. Mater. Interfaces. **8**, 5679–5686 (2016)
13. S. Tian, S. Li, J. Zhou, F. Xue, R. Cao, F. Wang, Effect of indium addition on interfacial IMC growth and bending properties of eutectic Sn-0.7Cu solder joints. J. Mater. Sci. Mater. Electron. **28**, 16120–16132 (2017)
14. B. Guo, A. Kunwar, N. Zhao, J. Chen, Y. Wang, H. Ma, Effect of Ag3Sn nanoparticles and temperature on Cu6Sn5 IMC growth in Sn-xAg/Cu solder joints. Mater. Res. Bull. **99**, 239–248 (2018)
15. J. Tian, P. Dai, X. Li, Interfacial reactions between Cu and Zn20Sn solder doped with minor RE. J. Mater. Sci. Mater. Electron. **28**, 17185–17192 (2017)
16. G. Chen, L. Liu, V.V. Silberschmidt, C. Liu, F. Wu, Y. Chan, Microstructural evolution of 96.5Sn-3Ag-0.5 Cu lead free solder reinforced with nickel-coated graphene reinforcements under large temperature gradient. J. Mater. Sci. Mater. Electron. (2018). https://doi.org/10.1007/s10854-017-8489-7
17. F. Wang, X. Ma, Y. Qian, Improvement of microstructure and interface structure of eutectic Sn–0.7 Cu solder with small amount of Zn addition. Scr. Mater. **53**, 699–702 (2005)
18. Y. Wang, Y. Lin, C. Tu, C. Kao, Effects of minor Fe, Co, and Ni additions on the reaction between SnAgCu solder and Cu. J. Alloys Compd. **478**, 121–127 (2009)
19. Y. Liu, J. Meerwijk, L. Luo, H. Zhang, F. Sun, C.A. Yuan, G. Zhang, Formation and evolution of intermetallic layer structures at SAC305/Ag/Cu and SAC0705-Bi-Ni/Ag/Cu solder joint interfaces after reflow and aging. J. Mater. Sci. Mater. Electron. **25**, 4954–4959 (2014)
20. X. Hu, Y. Chan, K. Zhang, K. Yung, Effect of graphene doping on microstructural and mechanical properties of Sn-8Zn-3Bi solder joints together with electromigration analysis. J. Alloys Compd. **580**, 162–171 (2013)
21. L. Xu, L. Wang, H. Jing, X. Liu, J. Wei, Y. Han, Effects of graphene nanosheets on interfacial reaction of Sn–Ag–Cu solder joints. J. Alloys Compd. **650**, 475–481 (2015)
22. Y. Liu, F. Sun, H. Zhang, P. Zou, Solderability, IMC evolution, and shear behavior of low-Ag Sn0.7Ag0.5Cu-BiNi/Cu solder joint. J. Mater. Sci. Mater. Electron. **23**, 1705–1710 (2012)
23. F. Cheng, F. Gao, H. Nishikawa, T. Takemoto, Interaction behavior between the additives and Sn in Sn-3.0Ag-0.5 Cu-based solder alloys and the relevant joint solderability. J. Alloys Compd. **472**, 530–534 (2009)
24. S. Chen, L. Brown, M. Levendorf, W. Cai, S.-Y. Ju, J. Edgeworth, X. Li, C.W. Magnuson, A. Velamakanni, R.D. Piner, Oxidation resistance of graphene-coated Cu and Cu/Ni alloy. ACS Nano **5**, 1321–1327 (2011)
25. Y. Huang, Z. Xiu, G. Wu, Y. Tian, P. He, Sn-3.0Ag-0.5Cu nanocomposite solders reinforced by graphene nanosheets. J. Mater. Sci. Mater. Electron. **27**, 6809–6815 (2016)
26. Y. Liu, F. Sun, X. Li, Effect of Ni, Bi concentration on the microstructure and shear behavior of low-Ag SAC-Bi-Ni/Cu solder joints. J. Mater. Sci. Mater. Electron. **25**, 2627–2633 (2014)